(12) INTERNATIONAL APPLICATION PUBLISHED UNDER THE PATENT COOPERATION TREATY (PCT)

(19) World Intellectual Property Organization
International Bureau

(43) International Publication Date
18 June 2020 (18.06.2020)

WIPO | PCT

(10) International Publication Number
WO 2020/123919 A1

(51) International Patent Classification:
C09K 5/20 (2006.01) *C04B 35/583* (2006.01)
C01B 21/064 (2006.01)

(21) International Application Number:
PCT/US2019/066193

(22) International Filing Date:
13 December 2019 (13.12.2019)

(25) Filing Language: English

(26) Publication Language: English

(30) Priority Data:
62/779,544 14 December 2018 (14.12.2018) US

(71) Applicants: **THE PENN STATE RESEARCH FOUNDATION** [US/US]; 304 Old Main, University Park, Pennsylvania 16802 (US). **SHINSHU UNIVERSITY** [JP/JP]; Institute of Carbon Science & Technology, Shinshu University, Wakasato 4-17-1, Nagano-City, Nagano 380-8553 (JP).

(72) Inventors; and

(71) Applicants: **TERRONES, Mauricio** [US/US]; 2376 Sagamore Dr., State College, Pennsylvania 16803 (US). **LEI, Yu** [US/US]; 265 Blue Course Dr., Apt. G24, State College, Pennsylvania 16803 (US). **LIU, He** [US/US]; 425 Waupelani Dr., Apt. 519, State College, Pennsylvania 16801 (US). **FUJISAWA, Kazunori** [US/US]; 3704 Plaza Dr., State College, Pennsylvania 16801 (US). **ELIAS ARRIAGA, Ann Laura** [US/US]; 406 S. Corl St., Apt. 9, State College, Pennsylvania 16801 (US). **ZHANG, Tianyi** [US/US]; 425 Waupelani Dr., Apt. 504, State College, Pennsylvania 16801 (US). **CRUZ-SILVA, Eduardo** [US/JP]; c/o Shinshu University, Institute of Carbon Science & Technology, Shinshu University, Wakasato 4-17-1, Nagano-city, Nagano 380-8553 (JP). **ENDO, Moronobu** [JP/JP]; Shinshu University, Institute of Carbon Science & Technology, Shinshu University, Wakasato 4-17-1, Nagano-city, Nagano 380-8553 (JP).

(74) Agent: **STEWART III, Duane A.**; Buchanan Ingersoll & Rooney PC, Union Trust Building, 501 Grant Street, Suite 200, Pittsburgh, Pennsylvania 15219 (US).

(54) Title: REDUCTIVE BORON NITRIDE WITH EXTENDED REACTIVE VACANCIES FOR CATALYTIC APPLICATIONS

FIG. 1

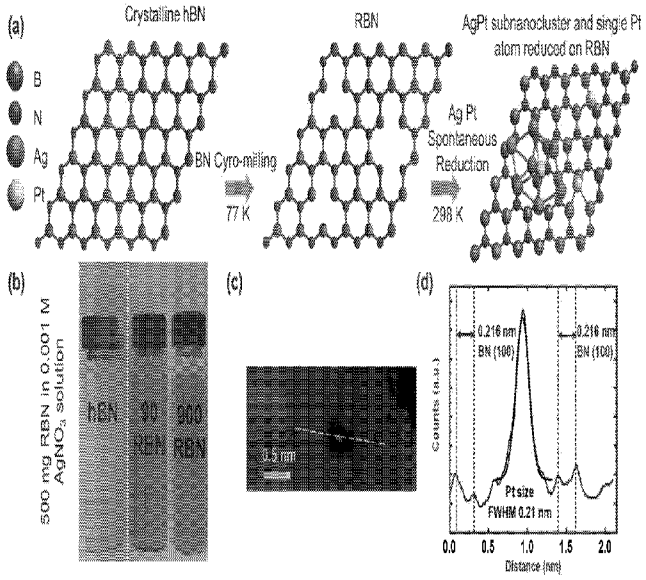

(57) **Abstract:** A group of reductive 2D materials (R2D) with extended reactive vacancies and a method for making the R2D materials with extended reactive vacancies are provided, the primary example being reductive boron nitride (RBN). To create defects such as vacancies, boron nitride (BN) powders are milled at cryogenic temperatures. The oxidation and powder agglomeration are significantly suppressed under these conditions, so that structural defects including points and triangular vacancies are retained without the formation of boron oxide.

WO 2020/123919 A1

[Continued on next page]

(81) **Designated States** *(unless otherwise indicated, for every kind of national protection available)*: AE, AG, AL, AM, AO, AT, AU, AZ, BA, BB, BG, BH, BN, BR, BW, BY, BZ, CA, CH, CL, CN, CO, CR, CU, CZ, DE, DJ, DK, DM, DO, DZ, EC, EE, EG, ES, FI, GB, GD, GE, GH, GM, GT, HN, HR, HU, ID, IL, IN, IR, IS, JO, JP, KE, KG, KH, KN, KP, KR, KW, KZ, LA, LC, LK, LR, LS, LU, LY, MA, MD, ME, MG, MK, MN, MW, MX, MY, MZ, NA, NG, NI, NO, NZ, OM, PA, PE, PG, PH, PL, PT, QA, RO, RS, RU, RW, SA, SC, SD, SE, SG, SK, SL, SM, ST, SV, SY, TH, TJ, TM, TN, TR, TT, TZ, UA, UG, US, UZ, VC, VN, ZA, ZM, ZW.

(84) **Designated States** *(unless otherwise indicated, for every kind of regional protection available)*: ARIPO (BW, GH, GM, KE, LR, LS, MW, MZ, NA, RW, SD, SL, ST, SZ, TZ, UG, ZM, ZW), Eurasian (AM, AZ, BY, KG, KZ, RU, TJ, TM), European (AL, AT, BE, BG, CH, CY, CZ, DE, DK, EE, ES, FI, FR, GB, GR, HR, HU, IE, IS, IT, LT, LU, LV, MC, MK, MT, NL, NO, PL, PT, RO, RS, SE, SI, SK, SM, TR), OAPI (BF, BJ, CF, CG, CI, CM, GA, GN, GQ, GW, KM, ML, MR, NE, SN, TD, TG).

Published:

— *with international search report (Art. 21(3))*

REDUCTIVE BORON NITRIDE WITH EXTENDED REACTIVE VACANCIES FOR CATALYTIC APPLICATIONS

CROSS-REFERENCE TO RELATED APPLICATIONS

This application claims the benefit of United States Provisional Patent Application No. 62/779,544, filed on December 14, 2018, which is incorporated by reference in its entirety.

BACKGROUND OF THE INVENTION

Field of the Invention

The present invention relates to catalytic materials that use reductive boron nitride.

Background of the Related Art

Reductive two-dimensional (2D) material is a type of 2D material with chemical reactive sites generated by cryo-milling. For example, reductive boron nitride (RBN) is a defective hexagonal boron nitride (hBN) with chemical reactive sites that are randomly distributed on the surface and are capable of reducing metal compounds to their lower oxidation states including but not limited to metallic clusters and single atoms. Although hBN itself is rarely considered as a promising catalyst, its excellent chemical stability, high thermal conductivity, and large band gap of 5.5 eV make it a strong candidate as a catalyst support under various harsh conditions (e.g., high temperature, acid, and base). (Uosaki, K. *et al.* "Boron Nitride Nanosheet on Gold as an Electrocatalyst for Oxygen Reduction Reaction: Theoretical Suggestion and Experimental Proof," *J. Am. Chem. Soc.* 136, 6542-6545, doi:10.1021/ja500393g (2014).) By introducing defects such as vacancies and hetero-atoms, hBN can be activated into RBN so that the optical bandgap is reduced to ~1.9 eV and various defect levels are created within the forbidden gap. (Tran, T. T., *et al.*, "Quantum emission from hexagonal boron nitride monolayers," *Nat. Nanotechnol.* 11, 37-+, doi:10.1038/nnano.2015.242 (2016); Weng, Q. H. *et al.* "Tuning of the Optical, Electronic, and Magnetic Properties of Boron Nitride Nanosheets with Oxygen Doping and Functionalization," *Adv. Mater.* 29, doi:10.1002/adma.201700695 (2017). Attaccalite, C., et al., "Coupling of excitons and defect states in boron-nitride nanostructures," *Phys. Rev.* B 83, 7, doi:10.1103/PhysRevB.83.144115 (2011). The changes in the band structure in RBN allows the charge transfer between BN and metal cations to happen so that metal cations can

be spontaneously reduced at the BN surface. (Sun, Y. G., "Metal Nanoplates on Semiconductor Substrates," *Advanced Functional Materials* 20, 3646-3657, doi:10.1002/adfm.201001336 (2010)). In addition, theoretical calculations have demonstrated that vacancy-defects such as B-, N-, B+V vacancies are favorable sites for metal (Pt, Ni, Ag) nucleation, which results in a robust bond between the reduced metal and the support at the vacancy-rich area. (Xu, D., et al., "Theoretical Study of the Deposition of Pt Clusters on Defective Hexagonal Boron Nitride (h-BN) Sheets: Morphologies, Electronic Structures, and Interactions with 0," *J. Phys. Chem.* C 118, 8868-8876, doi:10.1021/jp4087943 (2014); Lu, Z. S. *et al.* "A promising single atom catalyst for CO oxidation: Ag on boron vacancies of h-BN sheets," *Phys. Chem. Chem. Phys.* 19, 16795-16805, doi:10.1039/c7cp02430d (2017); Preobrajenski, A. B. *et al.*, "Adsorption-induced gap states of h-BN on metal surfaces," *Phys. Rev.* B 77, 5, doi:10.1103/PhysRevB.77.085421 (2008)). Furthermore, due to the inertness of defect-free BN regions, the growth of the metal is confined near the defects, giving rise to the formation of the single metal atom and sub-nanoclusters without migration and aggregation.

BRIEF SUMMARY OF THE INVENTION

One aspect of the present invention is directed to a reductive boron nitride (RBN). RBN is a defective hexagonal boron nitride with chemical reactive sites that are randomly distributed on its surface. The chemical reactive sites are configured for reducing metal compounds and single metal atoms to their lower oxidation states.

In one embodiment, the metal compounds and metal atoms include Pt, Au, Ag, Pd, Fe, Co, and Ni, and any combinations thereof.

In another embodiment, the chemical reactive sites are lattice imperfections.

In another embodiment, the lattice imperfections are extended reactive vacancies, reactive edges and other distortions.

In another embodiment, the chemical reactive sites have reactive edges and the average lateral size of the reactive edges is from 400 pm to 10 micrometers.

In another embodiment, the chemical reactive sites have extended reactive vacancies and the average diameter of the extended reactive vacancies is from 170 pm to 50 nm.

In another embodiment, the chemical reactive sites have extended reactive vacancies, and the extended reactive vacancies are configured for reducing the bandgap of hexagonal boron nitride (hBN) from insulating boron nitride (BN) to semiconducting RBN.

In another embodiment, the bandgap of the insulating BN is from 5 to 6 eV, and the bandgap of the semiconducting RBN is from 0.1 to 4.99 eV.

In another embodiment, the chemical reactive sites have extended reactive vacancies, and the extended reactive vacancies are configured for emitting photons with energies ranging from 315 nm to 1400 nm.

In another embodiment, the average particle size of the RBN is less than 10 μm, and the surface area of the RBN is greater than 30 m^2/g.

In another embodiment, the extended reactive vacancies are configured to reduce and anchor metal atoms and metal compounds in/on the reductive boron nitride lattice to form a metal nanostructure decorated RBN.

In another embodiment, the metal nanostructure decorated RBN includes an isolated single atom, few-atom clusters with an average size ranging from 175 pm to 1 nm, nanoparticles with an average size ranging from 1 nm to 500 nm, and any combination thereof.

In another embodiment, the metal atom is used in a catalytic application. The catalytic application includes a hydrogen evolution reaction, an oxygen evolution reaction, an oxygen reduction reaction, an acetylene cyclotrimerization, a HCHO oxidation, a methanol oxidation, a CO oxidation, and a CO_2 reduction.

Another aspect of the present invention is directed to a method for making reductive boron nitride (RBN) with extended reactive vacancies. The method includes mechanical grinding of hexagonal boron nitride at a cryogenic temperature to create extended reactive vacancies.

In one embodiment, the grinding time is longer than 0 min.

In another embodiment, the cryogenic temperature is at or below 123 K.

In another embodiment, the mechanical grinding is conducted in containers with one or more movable impactors.

Another aspect of the present invention is directed to a method for making metal decorated reductive boron nitride (RBN) with extended reactive vacancies. The method includes a) mixing the RBN with extended reactive vacancies with a metal precursor in a polar or non-polar solvent or solvents at room temperature; b) washing away excess metal compounds with polar or non-polar solvent or solvents by centrifugation or filtration; and c) re-dispersing materials obtained from b) in polar or non-polar solvent or solvents. The obtained liquid suspensions can be used as is or as powders after evaporating the solvent or solvents.

In one embodiment, the metal is selected from all metals, and any combination thereof.

In another embodiment, the metals are in ionic form and the ionic form includes Ag^{+}, Pt^{4+}, Au^{3+} in the obtained liquid suspensions.

In another embodiment, the solvent or solvents of the obtained liquid suspension is selected from the group consisting of polar and non-polar solvents, and the solvent includes ethanol, isopropanol, hexane, acetone, and any combination thereof..

Other aspects and advantages of the invention will be apparent from the following description, drawings and the appended claims.

BRIEF DESCRIPTION OF THE DRAWINGS

FIG. 1. (a) Schematic illustration of the synthesis of single atom Pt and few atoms AgPt clusters reduced on/by RBN. (b) The photograph of 500 mg hBN and RBN (90 and 900 min) after the reaction with 10 ml 0.001 M $AgNO_3$ aqueous solution at room temperature. (c) HAADF-STEM image of single Pt atom on 90RBN (90RBN-Pt) with higher magnification. (d) Line profile from the white dashed line in (c).

FIG. 2. (a) XRD spectra of hBN and RBN with different cryo-milling time (90 and 900 min). (b) N_2 adsorption and desorption isotherms of hBN, 90RBN, and 900RBN. (c-d) HRTEM image of the 90RBN, (c) showing the defects at the edges; (d) the triangular and point vacancies.

FIG. 3. Room-temperature photoluminescence spectra of 90RBN at 3 different sites with a 488 nm excitation laser. Emissions at 1.66, 1.75, 1.79, 1.82, 1.95, 2.05, and 2.10 eV can be found.

FIG. 4. (a) The HER polarization curves of 90RBN, 90RBN-Pt and 90RBN-Ag_1Pt_1. (b) Durability measurement of the 90RBN-Ag_1Pt_1. The polarization curves were recorded at the 1st cycle, and after 3000 cycles. The insets show the durability of 90RBN-Pt which fails after 3000 cycles.

FIG. 5. Onset potential vs. Tafel slope of this work and other published HER catalysts.

FIG. 6. Cost estimation (upper axis) based on Pt price (USD 31.34 per g) in January 2018, the Pt loading (lower axis), and the HER current density (constant overpotential η=80 mV) among 90 min RBN-Ag_1Pt_1 obtained experimentally (star), and various Pt catalysts (triangles and circles) calculated using the Tafel equation; Thin films (triangles; thickness given, 1 ML and 4 ML represents 1 monolayer and 4 layers, respectively). Spherical particles (circles; diameter in nm; at 20 mA cm^{-2} and 100 mA cm^{-2}).

FIG. 7. HRTEM images of (a)RBN and (b) RBN-Au.

FIG. 8. (a) XRD diffraction pattern for the pristine WS_2 and WS_2 cryomilled samples. (b) WS_2 particle size calculated by Scherrer equation. (c) WS_2 dispersions in acetone prepared with the pristine WS_2, and with the cryomilled samples for 15, 30, and 45 min after 2 h of sonication (0.8 mg/mL). At the right of each sample is the corresponding WS_2 film deposited on a FTO electrode.

FIG. 9. XRD diffraction pattern for the pristine MoS_2 and MoS_2 cryomilled samples.

FIG. 10. (a) Raman spectra and the (b) XRD diffraction pattern of graphite, 1 h, 2 h, and 3 h cryo-milled graphite.

FIG. 11. Raman spectra of graphite, boron nitride, and graphite/BN mixture after 2h cryo-milling.

FIG 12. XRD diffraction pattern for cryomilled MoS_2 and cryomilled MoS_2/WS_2 mixture

FIG 13. Raman spectra of cryomilled MoS_2 and cryomilled MoS_2/WS_2 mixture

FIG 14. N_2 adsorption and desorption isotherms of pristine and cryomilled MoS2

FIG 15. HRTEM images of cryomilled MoS_2/WS_2 mixture

FIG 16. (a) The HER polarization curves of cryomilled MoS_2/WS_2 mixture. (b) Tafel slope of cryomilled MoS_2/WS_2 mixture. (c) The HER polarization curves of cryomilled MoS_2/WS_2 mixture with Pt functionalization. (d) Tafel slope of cryomilled MoS_2/WS_2 mixture Pt functionalization.

DETAILED DESCRIPTION OF THE INVENTION

Definitions

While the terms used herein are believed to be well understood by one of ordinary skill in the art, definitions are set forth herein to facilitate explanation of the subject matter disclosed herein.

Unless defined otherwise, all technical and scientific terms used herein have the same meaning as commonly understood by one of ordinary skill in the art to which the subject matter disclosed herein belongs. Although any methods, devices, and materials similar or equivalent to those described herein can be used in the practice or testing of the presently disclosed subject matter, representative methods, devices, and materials are described herein.

The terms “a,” “an,” and “the” refer to “one or more” when used in this application, including the claims. The use of the word “a” or “an” when used in conjunction with the term “comprising” in the claims and/or the specification may mean “one,” but it is also consistent with the meaning of “one or more,” “at least one,” and “one or more than one.”

All references to singular characteristics or limitations of the present disclosure shall include the corresponding plural characteristic(s) or limitation(s) and vice versa, unless otherwise specified or clearly implied to the contrary by the context in which the reference is made.

All combinations of method or process steps as used herein can be performed in any order, unless otherwise specified or clearly implied to the contrary by the context in which the referenced combination is made.

The methods and devices of the present disclosure, including components thereof, can comprise, consist of, or consist essentially of the essential elements and limitations of the embodiments described herein, as well as any additional or optional components or limitations described herein or otherwise useful.

Unless otherwise indicated, all numbers expressing physical dimensions, quantities of ingredients, properties such as reaction conditions, and so forth used in the specification and claims are to be understood as being modified in all instances by the term "about". Accordingly, unless indicated to the contrary, the numerical parameters set forth in this specification and claims are approximations that can vary depending upon the desired properties sought to be obtained by the presently disclosed subject matter.

As used herein, ranges can be expressed as from "about" one particular value, and/or to "about" another particular value. It is also understood that there are a number of values disclosed herein, and that each value is also herein disclosed as "about" that particular value in addition to the value itself. For example, if the value "10" is disclosed, then "about 10" is also disclosed. It is also understood that each unit between two particular units are also disclosed. For example, if 10 and 15 are disclosed, then 11, 12, 13, and 14 are also disclosed.

Example 1 Reductive Boron Nitride with Spontaneously Reduced Pt/AgPt for HER Catalyst

In the present invention, two-dimensional (2D) boron nitride (BN) with mechanically activated defects was selected as an ideal support to spontaneously reduce Pt single atom and AgPt subnanoclusters. Although BN itself is rarely considered as a promising catalyst, its excellent chemical stability, high thermal conductivity, and large band gap of 5.5 eV make it a strong candidate as catalyst support under various harsh conditions (e.g., high temperature, acid, and base). By introducing defects such as vacancies and hetero-atoms, BN can be activated to reductive boron nitride (RBN) so that the optical bandgap is reduced, and various defect levels are created within the forbidden gap. An RBN is a defective hexagonal boron nitride with chemical reactive sites that are randomly distributed on the surface and are

capable of reducing metal compounds to their lower oxidation states including but not limited to metallic clusters and single atoms.

To create defects, BN powders were cryo-milled at -196 °C for a certain time as shown in FIG. 1(a). A series of RBN with different cryo-milling time (90 and 900 min) were prepared. Then the reductive BN (RBN) was mixed with a various salt solution such as $AgNO_3$ aqueous solution at room temperature. Due to the reduction of Ag nanoparticles by RBN, the color of the powder is changed into blue in 90RBN and brown in 900RBN as shown in FIG. 1(b). Besides reducing Ag nanoparticles by RBN, atomically dispersed Pt atoms can also be spontaneously reduced by RBN, when the salt was changed $PtCl_4$. The line profile from the STEM image shown in FIG. 1(c-d) further confirms that single Pt atom with diameter 0.21 nm was reduced and embedded in BN lattice. Moreover, bimetallic AgPt subnanoclusters can also be reduced by RBN layer when switching the salt solution to the mixture of $AgNO_3$ and $PtCl_4$.

The reactivity from the RBN is attributed to the defects including edges and vacancies in RBN. The X-ray diffraction (XRD) in FIG. 2(a) shows a gradual disordering process when the cryo-milling time increases, as the BN (002) peak becomes weakened and broadened. As cryo-milling time increases, BN flakes were exfoliated by the shearing force from the milling, resulting in the decrease in the grain size and the particle size. Thus, more surfaces and edges were exposed, giving rise to the increase in the surface area. The N_2 sorption isotherms of the Hbn and RBN (90RBN and 900RBN) shown in FIG. 2(b) are classified as type II, indicating macropore solids, which is similar as that of exfoliated graphite. As cryo-milling time increases, the Brunauer-Emmer-Teller (BET) surface area and total pore volume increase from 37 $m^2 g^{-1}$ and 100 $mm^3 g^{-1}$ in hBN to 234 $m^2 g^{-1}$ and 516 $mm^3 g^{-1}$ in 900RBN, respectively. Besides the exposure of surfaces and edges via the exfoliation and the formation of smaller particles, the impact of milling also results in disordered structures, including exposed edges (FIG. 2(c)), and vacancies (point and triangular vacancies, FIG. 2(d)).

The introduced vacancies are also responsible for the created defect levels between the valence and conduction band of BN, giving rise to various photon emissions ranging from 1.59 to 2.19 eV^2. Room temperature photoluminescence spectra of 90RBN collected from 3 sites shown in FIG. 3 reveal the emissions at 1.66, 1.79, 1.82, 1.95, 2.05, and 2.10 eV. Among those, the most intense emission is at 1.95 eV in all three sites, and previous work has revealed that this emission is associated with the presence of nitrogen-vacancy along with a substitution of nitrogen at the boron site. The created defect states also enable the charge

transfer between the defective BN and the cations from the aqueous solution, so that Ag and Pt can be spontaneously reduced on the defective sites.

By reducing atomically dispersed Pt atoms and AgPt subnanoclusters on RBN, the compounds can be used as the catalyst for hydrogen evolution reaction (HER). The HER performance of RBN with atomically dispersed Pt and AgPt subnanoclusters (Ag_1Pt_1) was investigated in a 0.5 M H_2SO_4 solution. For an efficient HER catalyst, a high turnover frequency (TOF) and exchange current, and a low Tafel slope and onset potential are needed. The 90RBN (shown in FIG. 4(a)) exhibits negligible performance compared to the electrodes with Pt, indicating that only the atomically dispersed Pt atoms are HER active. In 90RBN-Pt where Pt atoms are atomically dispersed on BN, the onset potential is 31 mV that is comparable to commercialized Pt/C, and the Tafel slope is 47 mV dec^{-1}. Normally, the HER on Pt surface undergoes the Volmer-Tafel reaction such that the rate-limiting step is the recombination step. However, in 90RBN-Pt, since single Pt atoms are isolated by inert BN, the recombination of chemisorbed hydrogen atoms becomes sluggish, resulting in a relatively higher Tafel slope in 90RBN-Pt compared to that of commercialized Pt/C. The HER performance can be improved by forming bimetallic AgPt subnanoclusters. When the Ag to Pt molar ratio is 1 to 1 (90RBN-Ag_1Pt_1), the best HER performance can be achieved with an onset potential of 15 mV and a Tafel slope of 16 mV dec^{-1}. The exchange current of atomically dispersed Pt is 2 to 3 times higher than that of Pt in bulk form. TOF and exchange current reveal the intrinsic electrocatalytic activity per Pt atoms and the rate of hydrogen evolution per surface area at equilibrium, respectively. Hence, the improvements in TOFs and exchange current over Pt-based SACs further imply that the single atom catalyst (SAC) is designed to maximize the utilization of each metal atom which is counted as the active site, resulting in cost efficiency. The lifetime of the best performing catalyst 90RBN-Ag_1Pt_1 was evaluated in FIG. 4(b). FIG. 4(b) demonstrates that after 3000 cycles the performance is comparable to that of the 1st cycle, indicating that AgPt clusters are robustly anchored on defective BN. Compared to other reported HER catalysts in terms of Tafel slope and onset potential, 90RBN-Ag_1Pt_1 is the most robust and efficient HER catalyst with the smallest Tafel slope and onset potential (FIG. 5).

The cost of Pt is estimated and compared with other Pt nanostructures in FIG. 6 and the cost can be reduced by downsizing the particle sizes into nanostructures. Specifically, the Pt price is almost 1000 times lower in single Pt atom/sub-nanoclusters or monolayer Pt when compared to 100 nm diameter Pt particles or a 100 nm thick film. By forming 90RBN-Ag_1Pt_1, the estimated cost is close to the reported Pt monolayer, but the current density is 10

times higher. Thus, by synthesizing atomically dispersed Pt within Ag, the efficiency in terms of cost and performance can be maximized.

Example 2 Au reduction using reductive boron nitride (RBN)

In order to spontaneously reduce Au nanoparticles on RBN, a Au(I) solution was first prepared by mixing 0.5 mL 0.01 M Au(III) tetrachloroaurate with 50 μL 0.005 M ascorbic acid and 9.45 mL DI water to form a colorless solution. Then, RBN was added into the prepared Au(I) solution. After a 10 min stirring, the solids were separated by centrifugation, followed by DI water washing and drying. The dried powder was characterized by high-resolution transmission electron microscopy (HRTEM). As disclosed in FIG. 7, Au particles with a diameter ~ 2-3 nm were spontaneously reduced on RBN, especially on the defective sites.

Example 3 Defective WS_2 via Cryo-milling

WS_2 (2 μm, 99%, Sigma-Aldrich) was milled in a solid state at a cryogenic temperature (~77.2 K) in a cryogenic mill SPEX 6770 Freezer/Mill. The cryogenic grinding process consisted of an oscillating steel impactor within a plastic vial, immersed in liquid nitrogen. Prior to the grinding process, each sample was pre-cooled for 10 minutes, and then cryo-milled with different time/cycles (10. 30. 45 min). Each milling cycle corresponds to 3 min grinding followed by 2 min of cooling.

After cryomilling, the samples were characterized by XRD. In FIG. 8(a) is shown an analysis of (002) peak, where the full width at half maximum (FWHM) of the normalized peak for the four samples was calculated. The peak area decrement for the longer cryomilled samples is related to the lattice deformation caused by atomic defects such as vacancies, dislocations, interstitial or substitutional atoms, and other defects caused by the cryomilling process. FIG. 8(b) presents the particle size obtained from calculations by the Scherrer equation and the corresponding FWHM (°) and milling time. The values indicate that cryomilling WS_2 powder for 45 min reduces approximately 40% its particle size.

Due to the lattice deformation and grain size reduction, cryo-milled WS_2 is easier to be dispersed in solution. Acetone dispersions of pristine WS_2, $15WS_2$, $30WS_2$ and $45WS_2$ (0.8 mg/mL) were prepared from the cryomilled powder by placing them under sonication for two hours and then pouring them into a 6 cm^3 cell leaving an electrode gap of 1 cm. The electrophoretic deposition was carried out by applying 60 V using a 2400 Keithley sourcemeter between two cleaned FTO on glass electrodes for 30 sec. The dispersions prepared with the samples milled for 15, 30 and 45 min have a difference in colloidal stability as compared to the dispersion prepared with pristine WS_2. It is expected that, as the particle

size decreases, the contribution of the Brownian motion plays a more important role in providing colloidal stability. FIG. 8(c) shows the resultant electrode after the electrophoretic deposition. The films show homogeneous deposition covering the substrate.

Example 4 Defective MoS_2 via Cryo-milling

Molybdenum disulfide (MoS_2) is a layered semiconductive transition metal dichalcogenide (TMD). The XRD pattern of pristine MoS_2 is characteristic for the hexagonal with the highest intensity reflection peak at d = 6.16 Å (002) as disclosed in FIG. 9. After cryo-milling, no obvious phase change can be obtained, but defects, edges, and more exposed area are created in MoS_2. After a 45 min cryo-milling, the grain size of MoS_2 decreased to 48.6 nm from 77.2 nm in pristine MoS_2. As shown in FIG 14 cryo-milling time increases, the BET surface area and total pore volume increase from 10.9 m^2/g and 38.2 mm^3/gin pristine MoS_2 to 24.8567 m^2/g and 52.5 $mm^3\ g^{-1}$ in 90min MoS_2, respectively. Due to the created defects, edges, and exposed edges, more dangling bonds are exposed as the reactive centers for molecular adsorption.

Example 5 Defective Graphite via Cryo-milling

Graphite is a layered conducting material. Similar to BN, WS_2, and MoS_2, defects, edges, and exposed surfaces can be obtained by cryo-milling. As disclosed in FIG. 10(a), I_D/I_G gradually increases as cryo-milling time increase, indicating an increased amount of the induced structural disorder *via* cryo-milling. The gradual shifts in 002 peak (see FIG. 10(b)) as cryo-milling time increases suggests the expanded layer distance after cryo-milling.

Example 6 Defective Graphite via Cryo-milling

The method can also be extended to the mixture of different 2D materials, for example, graphite and boron nitride mixture. Boron nitride and graphite were mixed before the cryo-milling. After 2 h cryo-milling, the mixture was well mixed, and defects were created. As disclosed in FIG. 11, Raman indicates the coexistence of boron nitride and graphite. In addition, the peak broadening implies that defects are presented in the mixture after the 2 h cryo-milling.

Although the present invention has been described in terms of specific exemplary embodiments and examples, it will be appreciated that the embodiments disclosed herein are for illustrative purposes only and various modifications and alterations might be made by those skilled in the art without departing from the spirit and scope of the invention as set forth in the following claims.

Documents reported herein are incorporated by reference in their entirety and do not carry an admission that they are prior art for any purpose. Where information specifically

stated in this specification can be construed to contradict anything in the incorporated material, the information specifically stated in this specification shall control.

Example 7 Defective MoS_2 and WS_2 mixture via Cryo-milling for HER catalyst

MoS_2 and WS_2 powders were also cryomilled together to form defective MoS_2 and WS_2 mixture. After 15-60 min cryo-milling, the powders were well mixed and defective. As seen in FIG 15, many step edges and defective sites are formed after 60min cryo-milling. Raman spectra was also applied to study the mixture and FIG 13 shows the co-existence of both MoS_2 and WS_2. Similar effect is also shown on the XRD spectra of MoS_2/WS_2 mixture shown in FIG 12. The defective sites in the mixture has also led to the enhanced HER catalytic performance. FIG 16 (a) and (b) shows the onset potential and Tafel slope of the cryo-milled mixture. The cryo-milling has also increased the chemical reactivity of the mixture which enables the mixture to spontaneous reduce $PtCl_4$ into Pt clusters which shows enhanced HER performances shown in FIG 16 (c) and (d).

CLAIMS

What is claimed is:

1. A reductive boron nitride (RBN), wherein the RBN is a defective hexagonal boron nitride with chemical reactive sites that are randomly distributed on its surface, and wherein the chemical reactive sites are configured for reducing metal compounds or single metal atoms to their lower oxidation states.
2. The RBN of claim 1, wherein the metal compounds and metal atoms comprise Pt, Au, Ag, Pd, Fe, Co, and Ni, and any combination thereof.
3. The RBN of claim 1, wherein the chemical reactive sites are lattice imperfections.
4. The RBN of claim 3, wherein the lattice imperfections are extended reactive vacancies or reactive edges.
5. The RBN of claim 1, wherein the chemical reactive sites have reactive edges, and wherein the average lateral size of the reactive edges is from 400 pm to 10 micrometers.
6. The RBN of claim 1, wherein the chemical reactive sites have extended reactive vacancies, and wherein the average diameter of the extended reactive vacancies is from 170 pm to 50 nm.
7. The RBN of claim 1, wherein the chemical reactive sites have extended reactive vacancies, and wherein the extended reactive vacancies are configured for reducing the bandgap of hexagonal boron nitride (hBN) from insulating boron nitride (BN) to semiconducting RBN.
8. The RBN of claim 7, wherein the bandgap of the insulating BN is from 5 to 6 eV, and the bandgap of the semiconducting RBN is from 0.1 to 4.99 eV.
9. The RBN of claim 1, wherein the chemical reactive sites have extended reactive vacancies, and wherein the extended reactive vacancies are configured for emitting photons with energies ranging from 315 nm to 1400 nm.
10. The RBN of claim 1, wherein the average particle size of the RBN is less than 10 μm, and the surface area of the RBN is greater than 30 m^2/g.
11. The RBN of any of claims 4 and 6-9, wherein the extended reactive vacancies are configured to reduce and anchor metal atoms and metal compounds in/on the RBN lattice to form a metal nanostructure decorated RBN.
12. The metal nanostructure-decorated RBN of claim 11, wherein the metal nanostructure decorated RBN comprises an isolated single atom, few-atom clusters with an average

size ranging from 175 pm to 1 nm, nanoparticles with an average size ranging from 1 nm to 500 nm, and any combination thereof.

13. The metal nanostructure decorated RBN of claim 11, wherein the metal atom is used in a catalytic application, wherein the catalytic application comprises a hydrogen evolution reaction, an oxygen evolution reaction, an oxygen reduction reaction, an acetylene cyclotrimerization, a HCHO oxidation, a methanol oxidation, a CO oxidation, and a CO_2 reduction.
14. A method for making reductive boron nitride (RBN) with extended reactive vacancies comprising mechanical grinding of hexagonal boron nitride at a cryogenic temperature to create extended reactive vacancies.
15. The method of claim 14, wherein the grinding time is longer than 0 min.
16. The method of claim 14, wherein the cryogenic temperature is at or below 123 K.
17. The method of claim 14, wherein the mechanical grinding is conducted in containers with one or more movable impactors.
18. A method for making metal nanostructure decorated reductive boron nitride (RBN) comprising:

    a) mixing RBN, wherein the RBN comprises extended reactive vacancies, with a metal precursor in a polar or non-polar solvent or solvents at room temperature;

    b) washing away excess metal compounds with polar or non-polar solvent or solvents by centrifugation or filtration; and

    c) re-dispersing materials obtained from b) in polar or non-polar solvent or solvents, wherein obtained liquid suspensions is used as is or as powders after evaporating the solvent or solvents.
19. The method of claim 18, wherein the metal is selected from all metals, and any combination thereof.
20. The method of claim 18, wherein the metals are in ionic form, and wherein the ionic form comprises Ag^{+}, Pt^{4+}, Au^{3+}in the obtained liquid suspensions.
21. The method of claim 18, wherein the solvent of the obtained liquid suspension is selected from the group consisting of polar and non-polar solvents, and wherein the solvent comprises ethanol, isopropanol, hexane, acetone, and any combination thereof.

FIG. 1

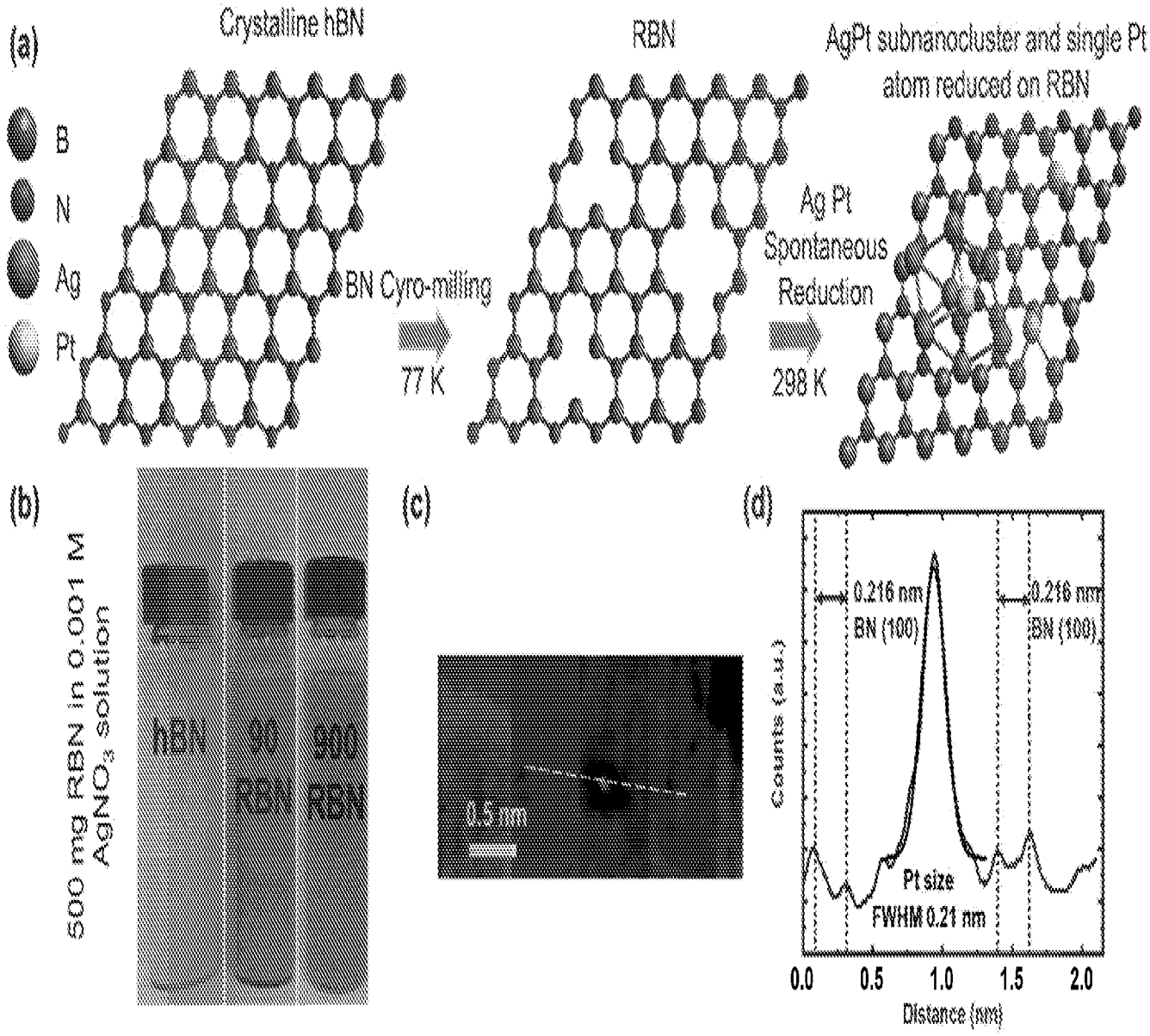
(a)
Crystalline hBN
RBN
AgPt subnanocluster and single Pt atom reduced on RBN
B
N
Ag
Pt
BN Cyro-milling
77 K
Ag Pt
Spontaneous
Reduction
298 K
(b)
500 mg RBN in 0.001 M AgNO3 solution
hBN
90 RBN
900 RBN
(c)
0.5 nm
(d)
0.216 nm
BN (100)
0.216 nm
BN (100)
Counts (a.u.)
Pt size
FWHM 0.21 nm
0.0
0.5
1.0
1.5
2.0
Distance (nm)

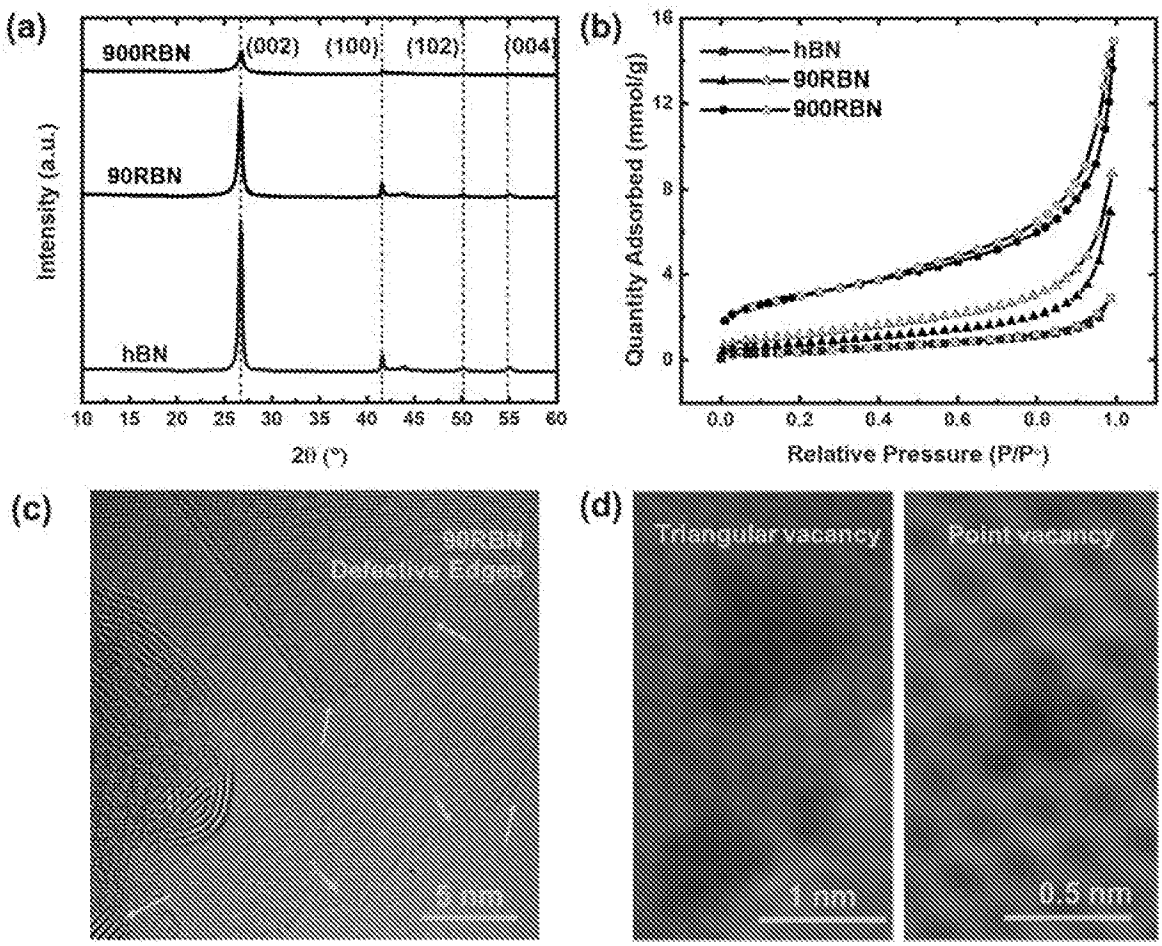
(a)
900RBN
90RBN
hBN
(002)
(100)
(102)
(004)
Intensity (a.u.)
10 15 20 25 30 35 40 45 50 55 60
2θ (°)
(b)
hBN
90RBN
900RBN
Quantity Adsorbed (mmol/g)
0 4 8 12 16
0.0 0.2 0.4 0.6 0.8 1.0
Relative Pressure (P/P°)
(c)
Grain
Boundary
5 nm
(d)
Triangular vacancy
1 nm
Point vacancy
0.5 nm

FIG. 2

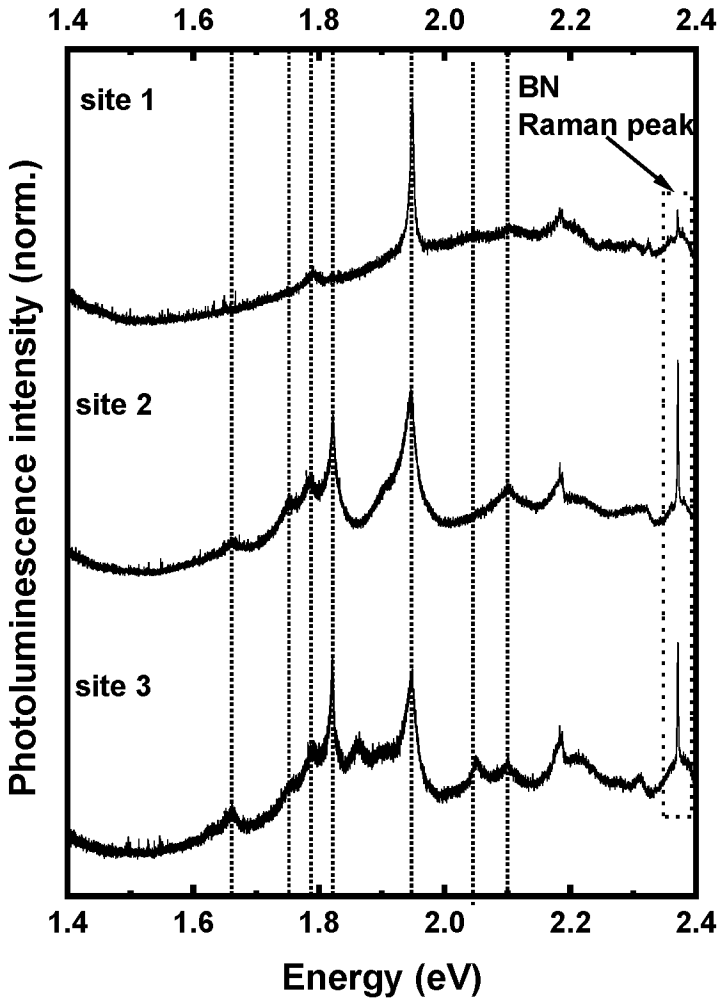
1.4
1.6
1.8
2.0
2.2
2.4
site 1
BN
Raman peak
site 2
site 3
Photoluminescence intensity (norm.)
Energy (eV)

FIG. 3

FIG. 4

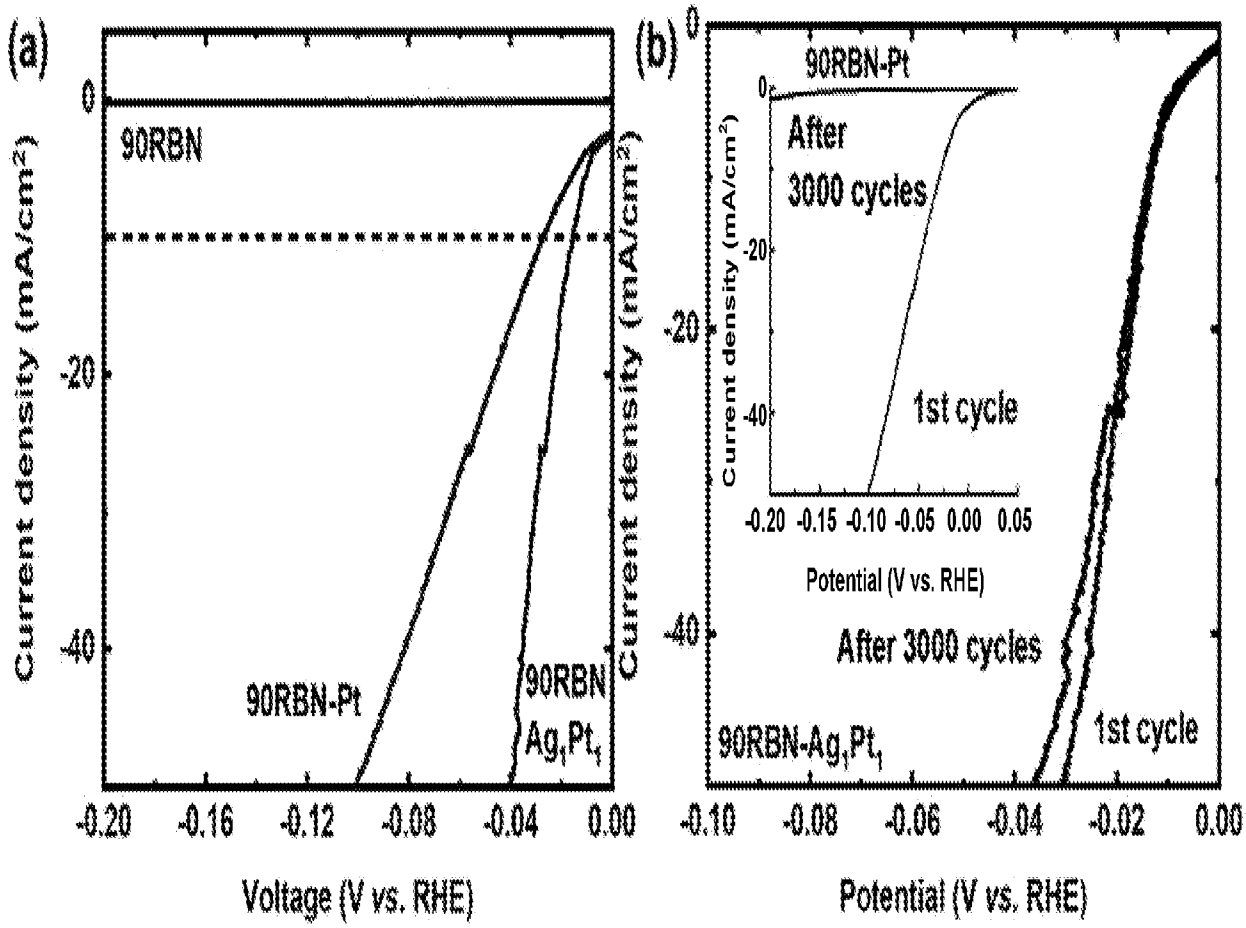
(a)
Current density (mA/cm²)
0
-20
-40
90RBN
90RBN-Pt
90RBN
Ag1Pt1
-0.20 -0.16 -0.12 -0.08 -0.04 0.00
Voltage (V vs. RHE)
(b)
Current density (mA/cm²)
0
-20
-40
90RBN-Pt
After
3000 cycles
1st cycle
-0.20 -0.15 -0.10 -0.05 0.00 0.05
Potential (V vs. RHE)
After 3000 cycles
90RBN-Ag1Pt1
1st cycle
-0.10 -0.08 -0.06 -0.04 -0.02 0.00
Potential (V vs. RHE)

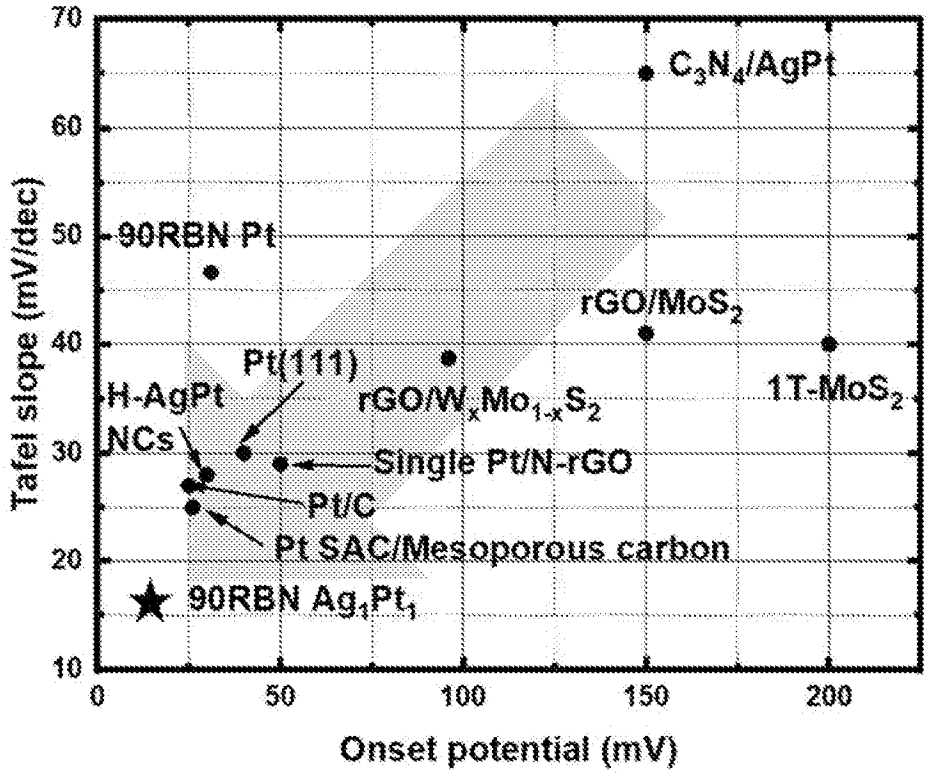
70
60
50
40
30
20
10
0
50
100
150
200
Tafel slope (mV/dec)
Onset potential (mV)
C3N4/AgPt
90RBN Pt
rGO/MoS2
1T-MoS2
Pt(111)
H-AgPt
NCs
rGO/WxMo1-xS2
Single Pt/N-rGO
Pt/C
Pt SAC/Mesoporous carbon
90RBN Ag1Pt1

FIG. 5

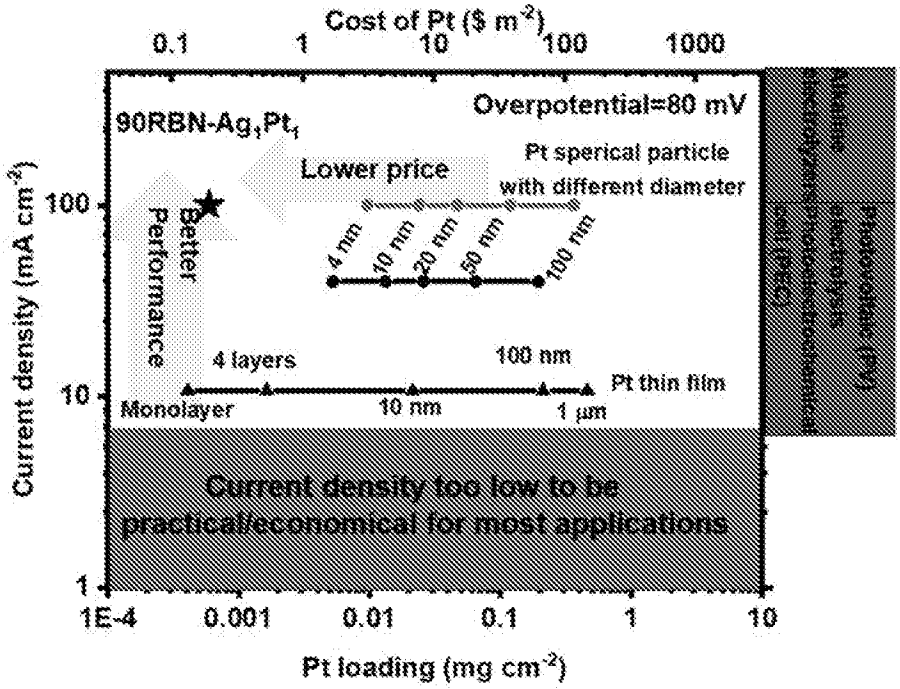
Cost of Pt ($ m-2)
0.1
1
10
100
1000
Overpotential=80 mV
90RBN-Ag1Pt1
Lower price
Pt sperical particle
with different diameter
4 nm
10 nm
20 nm
50 nm
100 nm
Better
Performance
4 layers
100 nm
Pt thin film
Monolayer
10 nm
1 μm
Current density too low to be
practical/economical for most applications
Current density (mA cm-2)
100
10
1
1E-4
0.001
0.01
0.1
1
10
Pt loading (mg cm-2)

FIG. 6

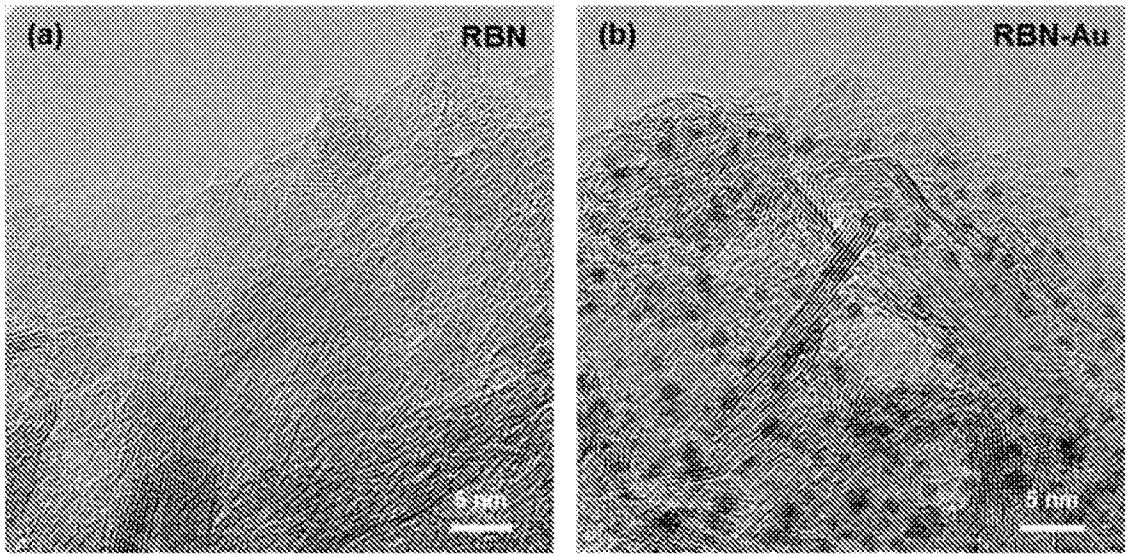

FIG. 7

FIG. 8

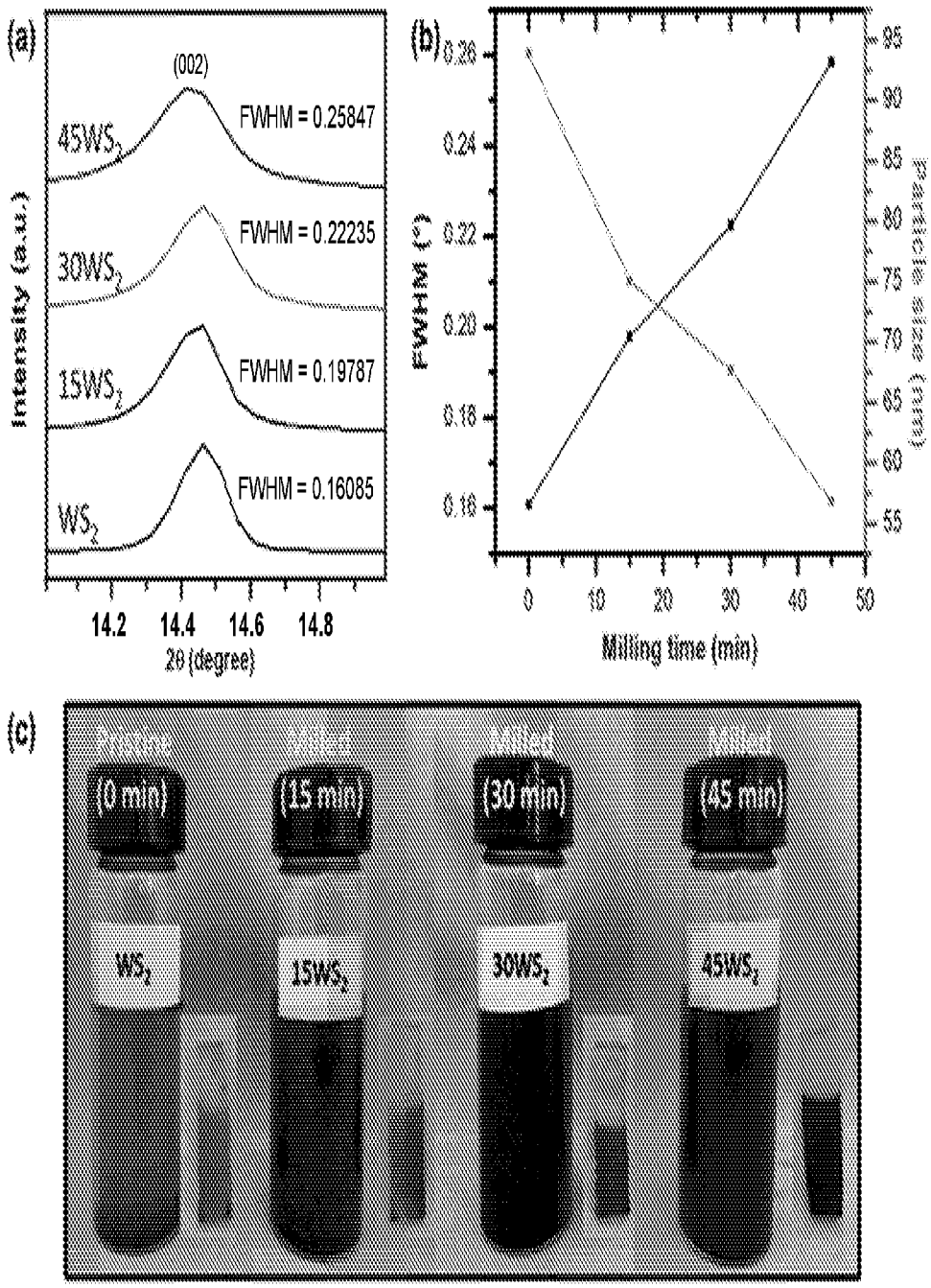
(a)
(002)
45WS2
FWHM = 0.25847
30WS2
FWHM = 0.22235
15WS2
FWHM = 0.19787
WS2
FWHM = 0.16085
Intensity (a.u.)
14.2
14.4
14.6
14.8
2θ (degree)
(b)
FWHM (°)
Particle size (nm)
Milling time (min)
(c)
Pristine
(0 min)
Milled
(15 min)
Milled
(30 min)
Milled
(45 min)
WS2
15WS2
30WS2
45WS2

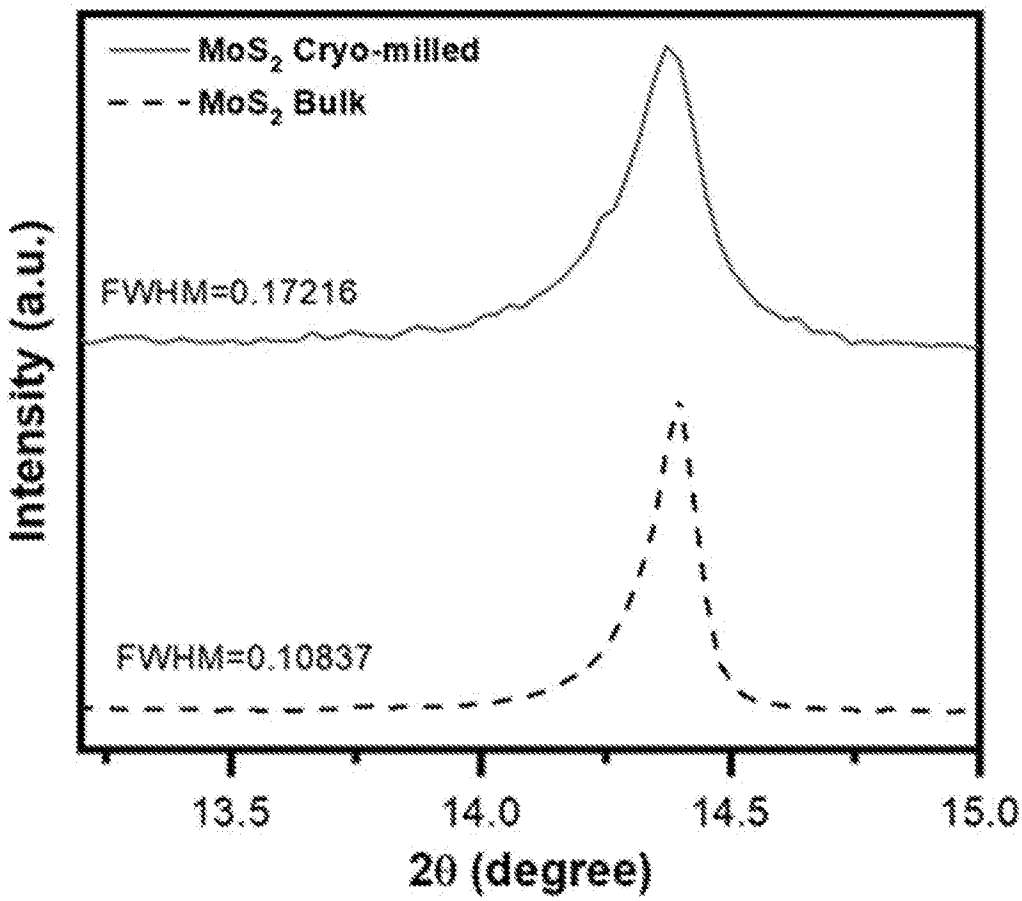
MoS2 Cryo-milled
MoS2 Bulk
FWHM=0.17216
FWHM=0.10837
Intensity (a.u.)
13.5
14.0
14.5
15.0
2θ (degree)

FIG. 9

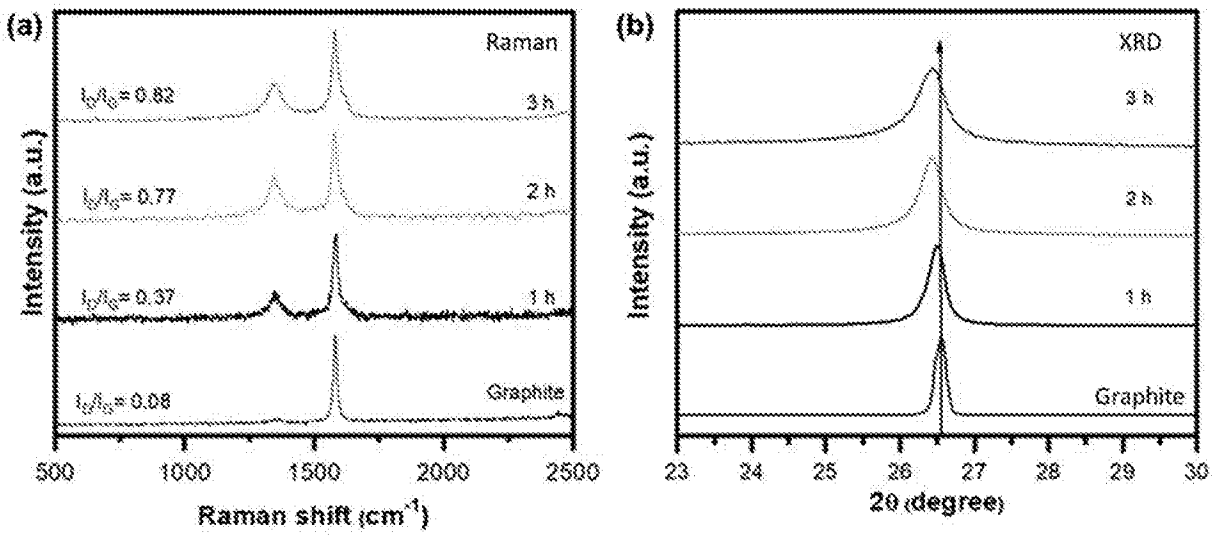
(a)
Raman
I_D/I_G = 0.82
3 h
I_D/I_G = 0.77
2 h
I_D/I_G = 0.37
1 h
I_D/I_G = 0.08
Graphite
Intensity (a.u.)
500
1000
1500
2000
2500
Raman shift (cm^{-1})
(b)
XRD
3 h
2 h
1 h
Graphite
Intensity (a.u.)
23
24
25
26
27
28
29
30
2θ (degree)

FIG. 10

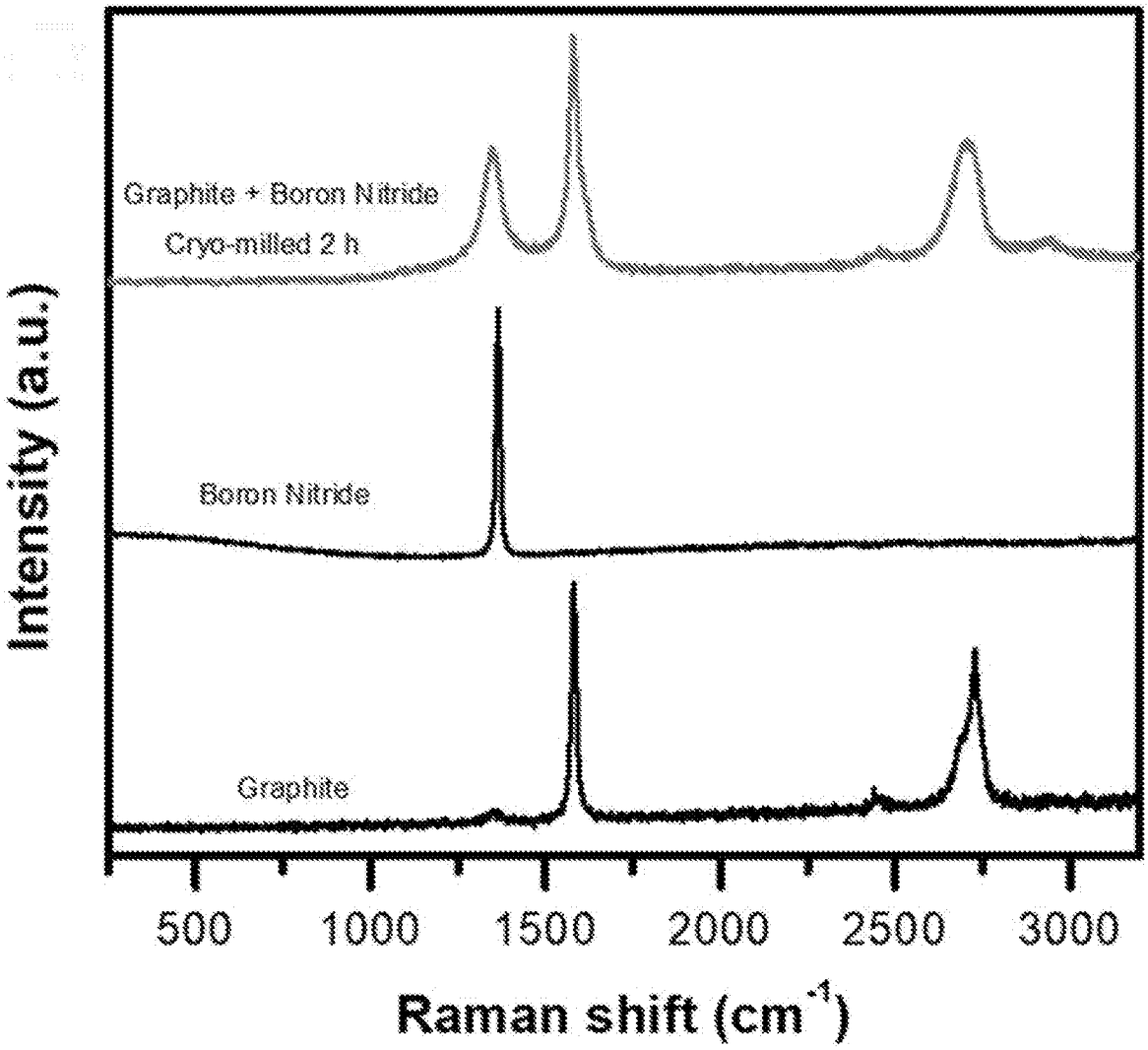
Graphite + Boron Nitride
Cryo-milled 2 h
Boron Nitride
Graphite
Intensity (a.u.)
500
1000
1500
2000
2500
3000
Raman shift (cm-1)

FIG. 11

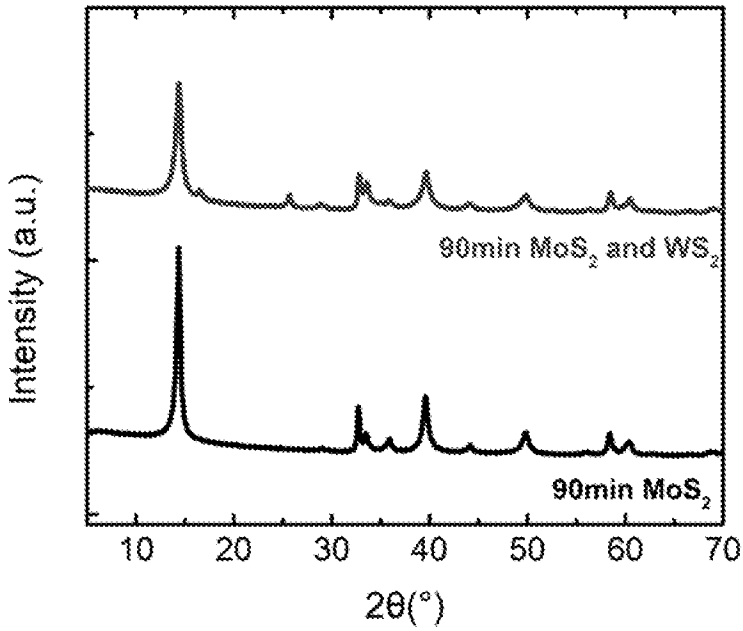
Intensity (a.u.)
90min MoS2 and WS2
90min MoS2
10
20
30
40
50
60
70
2θ(°)

FIG. 12

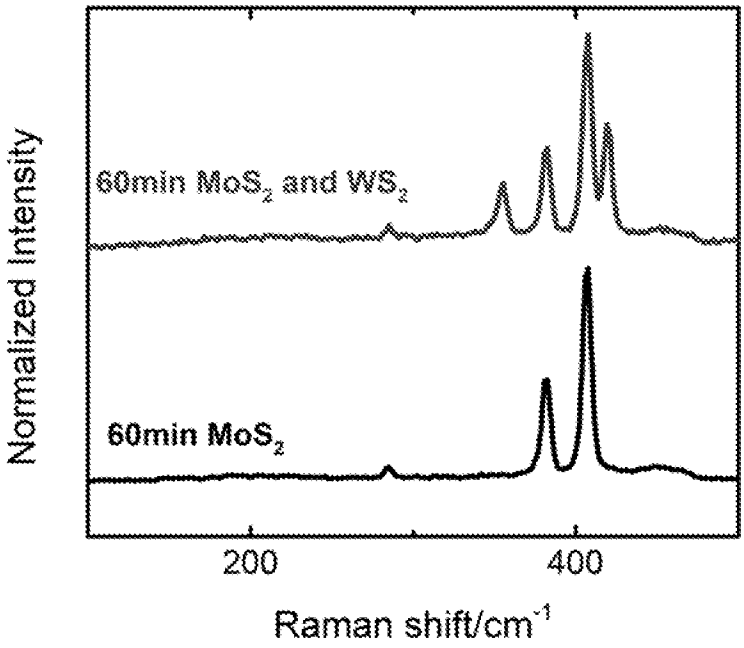
Normalized Intensity
60min MoS2 and WS2
60min MoS2
200
400
Raman shift/cm-1

FIG. 13

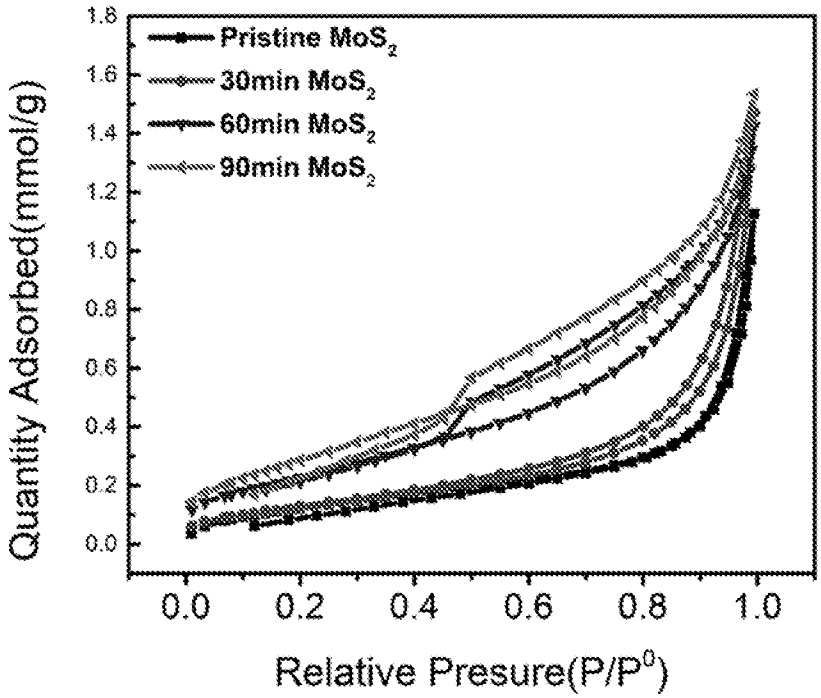
Pristine MoS2
30min MoS2
60min MoS2
90min MoS2
Quantity Adsorbed(mmol/g)
Relative Presure(P/P0)
0.0
0.2
0.4
0.6
0.8
1.0
1.2
1.4
1.6
1.8

FIG. 14

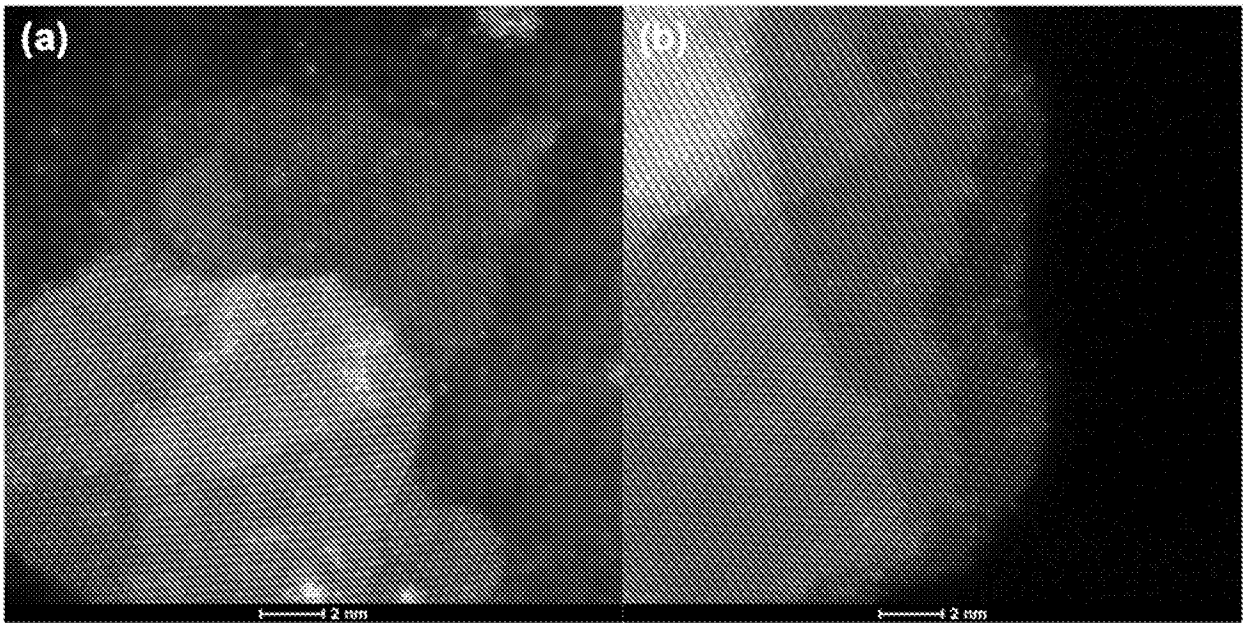

FIG. 15

FIG. 16

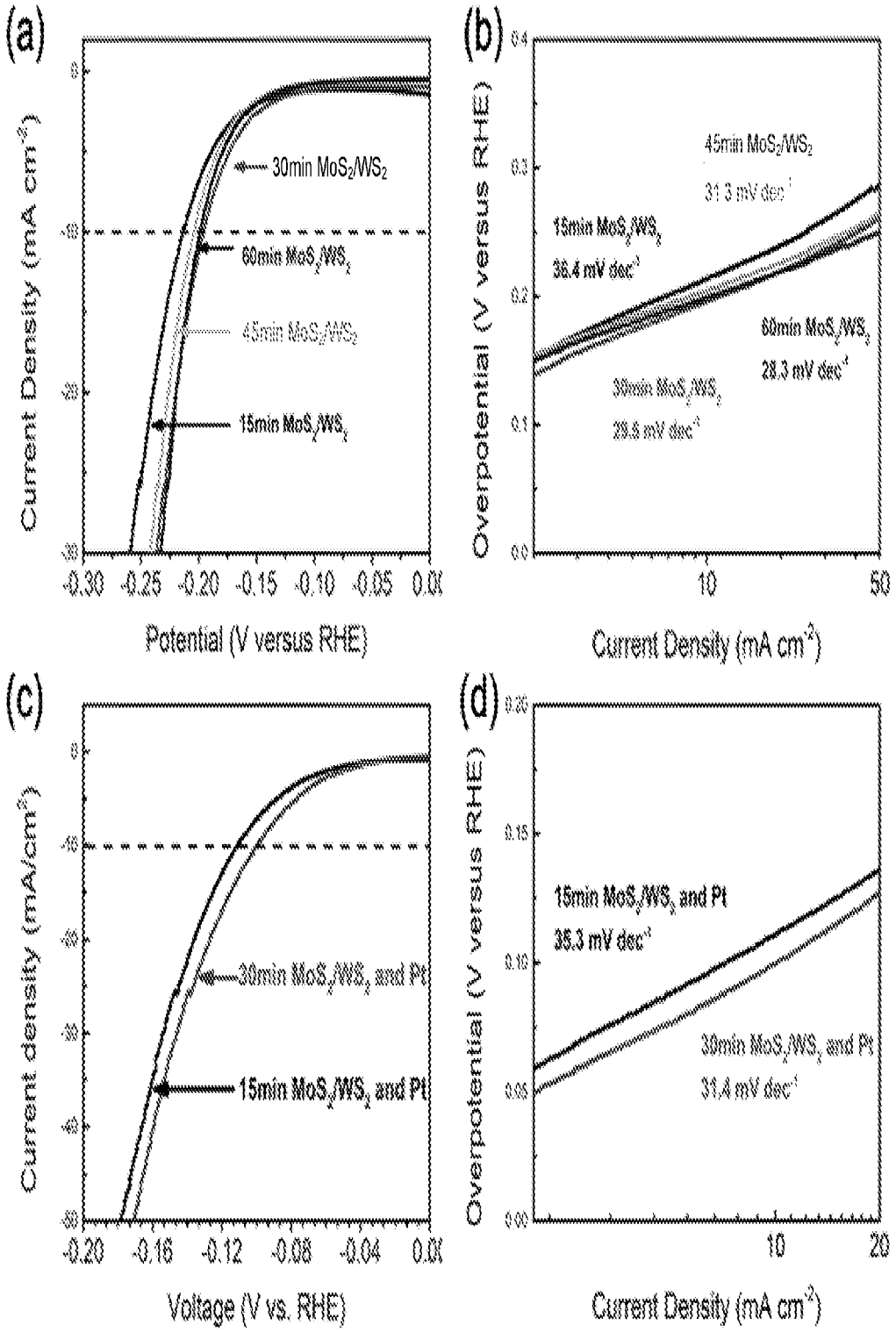
(a)
Current Density (mA cm-2)
30min MoS2/WS2
60min MoS2/WS2
45min MoS2/WS2
15min MoS2/WS2
-0.30 -0.25 -0.20 -0.15 -0.10 -0.05
Potential (V versus RHE)
(b)
Overpotential (V versus RHE)
45min MoS2/WS2
31.3 mV dec-1
15min MoS2/WS2
36.4 mV dec-1
60min MoS2/WS2
28.3 mV dec-1
30min MoS2/WS2
29.5 mV dec-1
0.0 0.1 0.2 0.3 0.4
10 50
Current Density (mA cm-2)
(c)
Current density (mA/cm2)
30min MoS2/WS2 and Pt
15min MoS2/WS2 and Pt
-0.20 -0.16 -0.12 -0.08 -0.04
Voltage (V vs. RHE)
(d)
Overpotential (V versus RHE)
15min MoS2/WS2 and Pt
35.3 mV dec-1
30min MoS2/WS2 and Pt
31.4 mV dec-1
0.00 0.05 0.10 0.15
10 20
Current Density (mA cm-2)

INTERNATIONAL SEARCH REPORT

International application No.
PCT/US 19/66193

A. CLASSIFICATION OF SUBJECT MATTER

IPC - C09K 5/20; C01B 21/064; C04B 35/583 (2020.01)

CPC - C09K 5/10; C01B 21/064; C01B 21/0648; C04B 35/583; C04B 35/62695

According to International Patent Classification (IPC) or to both national classification and IPC

B. FIELDS SEARCHED

Minimum documentation searched (classification system followed by classification symbols)
See Search History document

Documentation searched other than minimum documentation to the extent that such documents are included in the fields searched
See Search History document

Electronic data base consulted during the international search (name of data base and, where practicable, search terms used)
See Search History document

C. DOCUMENTS CONSIDERED TO BE RELEVANT

Category*	Citation of document, with indication, where appropriate, of the relevant passages	Relevant to claim No.
X ----- Y	NPL - Fu et al, "In-situ growth of metal nanoparticles on boron nitride nanosheets as highly efficient catalysts", Journal of Materials Chemistry A, 4(48), pg 19107-19115; November 2016 (11.2016) (retrieved from internet URL: https://pubs.rsc.org/en/content/articlelanding/2016/ta/c6ta06409d#!divAbstract), pg 19108, left col, para 3-4; pg 19110, left col, para 2-3; pg 19110, left col, para 5 to right col, para 1; pg 19110, right col, para 4; abstract; Fig. 1, 2B, 2D, 2F, 3A-3B; Fig. S3A-S3B, S4A, S5A	1-6, 10-12, 18-21 ---------- 7-9, 13
X	US 2016/0276056 A1 (GRAPHENE 3D LAB INC) 22 September 2016 (22.09.2016), para [0014], [0050], [0083], [0148], [0166])	14-17
Y	NPL-Zhao et al., "Single Mo atom Supported on Defective Boron Nitride Monolayer as an Efficient Electrocatalyst for Nitrogen Fixation: A Computational Study", J. Am. Chem. Soc. 2017, 139, 36, pg 12480-12487; 11 August 2017 (11.08.2017) (retrieved from internet URL: https://pubs.acs.org/doi/10.1021/jacs.7b05213), pg 12482, right col, para 3 to pg 12483, left col, para 1; pg 12483, left col, para 2; Fig. S4, Fig. S6.	7-8
Y	NPL-Tran et al., "Quantum emission from hexagonal boron nitride monolayers", Nat Nanotechnol. 2016 Jan; 11(1): pg 37-41. doi: 10.1038/nnano.2015.242. Epub 26 October 2015 (26.10.2015) (retrieved from internet URL: https://www.ncbi.nlm.nih.gov/pubmed/26501751), abstract	9

☒ Further documents are listed in the continuation of Box C. ☐ See patent family annex.

* Special categories of cited documents:
"A" document defining the general state of the art which is not considered to be of particular relevance
"D" document cited by the applicant in the international application
"E" earlier application or patent but published on or after the international filing date
"L" document which may throw doubts on priority claim(s) or which is cited to establish the publication date of another citation or other special reason (as specified)
"O" document referring to an oral disclosure, use, exhibition or other means
"P" document published prior to the international filing date but later than the priority date claimed
"T" later document published after the international filing date or priority date and not in conflict with the application but cited to understand the principle or theory underlying the invention
"X" document of particular relevance; the claimed invention cannot be considered novel or cannot be considered to involve an inventive step when the document is taken alone
"Y" document of particular relevance; the claimed invention cannot be considered to involve an inventive step when the document is combined with one or more other such documents, such combination being obvious to a person skilled in the art
"&" document member of the same patent family

Date of the actual completion of the international search	Date of mailing of the international search report
11 February 2020	09 MAR 2020
Name and mailing address of the ISA/US Mail Stop PCT, Attn: ISA/US, Commissioner for Patents P.O. Box 1450, Alexandria, Virginia 22313-1450 Facsimile No. 571-273-8300	Authorized officer Lee Young Telephone No. PCT Helpdesk: 571-272-4300

INTERNATIONAL SEARCH REPORT

International application No.
PCT/US 19/66193

C (Continuation). DOCUMENTS CONSIDERED TO BE RELEVANT

Category*	Citation of document, with indication, where appropriate, of the relevant passages	Relevant to claim No.
Y	NPL-Lu et al., "Pd1/BN as a promising single atom catalyst of CO oxidation: a dispersion-corrected density functional theory study", RSC Adv., 5, pg 84381-84388 (2015) (retrieved from internet URL: https://pubs.rsc.org/lv/content/articlelanding/2015/ra/c5ra14057a/unauth#!divAbstract), page 4 of 15, para 1; abstract; Fig. 1	13